Journal of Physics: Conference Series **723** (2016) 012024 doi:10.1088/1742-6596/723/1/012024

Trapped ion $^{88}Sr^{+}$ optical clock systematic uncertainties – AC Stark shift determination

GP Barwood, G Huang, SA King, HA Klein and P Gill

National Physical Laboratory, Teddington Middlesex TW11 0LW U.K.

E-mail: geoffrey.barwood@npl.co.uk

Abstract. A recent comparison between two trapped-ion $^{88}Sr^{+}$ optical clocks at the UK National Physical Laboratory demonstrated agreement to 4 parts in 10^{17}. One of the uncertainty contributions to the optical clock absolute frequency arises from the blackbody radiation shift which in turn depends on uncertainty in the knowledge of the differential polarisability between the two clocks states. Whilst a recent NRC measurement has determined the DC differential polarisability to high accuracy, there has been no experimental verification to date of the dynamic correction to the DC Stark shift. We report a measurement of the scalar AC Stark shift at 1064 nm with measurements planned at other wavelengths. Our preliminary result using a fibre laser at 1064 nm agrees with calculated values to within ~3%.

1. Introduction

Since the seventh symposium, there has been strong progress in the development of optical frequency standards based on both cold trapped atoms and ions. Both projected and measured clock reproducibilities are now in the low parts in 10^{17} to few parts in 10^{18} for a number of atom and ion systems and details are given elsewhere in these proceedings. One of the optical frequency standards under development at the UK National Physical Laboratory (NPL) is based on the $5s\ ^2S_{1/2} - 4d\ ^2D_{5/2}$ electric quadrupole transition in $^{88}Sr^{+}$ at 674 nm. A partial term scheme, showing the cooling lasers and clock transition is shown in figure 1. This transition is also being studied at the National Research Council (NRC) in Canada and at the VTT Technical Research Centre of Finland. At NPL, we have recently compared two optical frequency standards based on $^{88}Sr^{+}$ at 674 nm and shown agreement to within 4 parts in 10^{17} [1]. This measurement confirmed experimentally the projected uncertainty by the NRC [2]. Other NPL work has centred on improvements in real-time monitoring and control of the micromotion [3] and a study on the effect of magnetic field noise on clock frequency stability [4]. A key advantage of the $^{88}Sr^{+}$ system is the ability to operate the RF trap at a frequency where the second order Doppler and Stark shifts due to the micromotion cancel [5]. Reference [5] also includes a measurement of the DC differential polarisability that had previously been a limiting factor in the uncertainty of the $^{88}Sr^{+}$ optical standard. However, in order to obtain the blackbody shift coefficient from the DC differential polarisability, a small "dynamic correction" [6] is applied. Although this correction is small, there has been, to date, no direct experimental confirmation of the AC Stark shift theory used to estimate this correction. In these proceedings, we present our first measurements of the Stark shift at 1064 nm, using a 100-mW fibre laser and compare our result with the calculated shift.

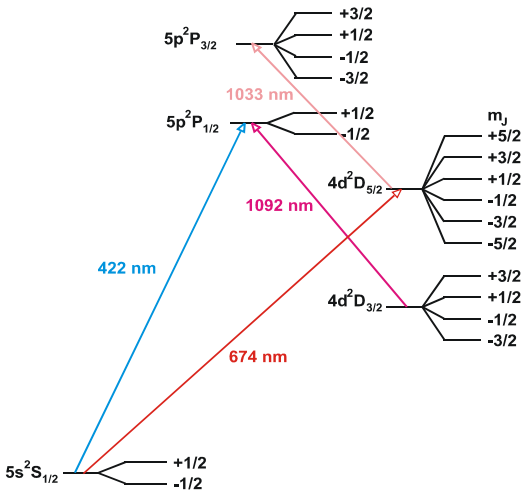

Figure 1. Partial term scheme for $^{88}Sr^+$, showing the wavelengths required to cool the ion, together with the 674 nm clock transition.

Figure 2 shows an overall schematic of our laser system, together with one of our two traps. Cooling light at 422 nm is provided by a frequency doubled 844-nm extended cavity laser, distributed feedback lasers provide the clear-out sources at 1033 nm and 1092 nm. Recently, VTT have demonstrated that these lasers can be replaced with amplified spontaneous emission sources [7], offering significant simplification. Full details of our laser system are given elsewhere [1, 3, 4]. Stark shift measurements are undertaken via two trap comparison with an additional laser directed into one of our two traps (figure 2). A computer-controlled shutter is used to accumulate data on the frequency shift with this laser shuttered "on" and "off".

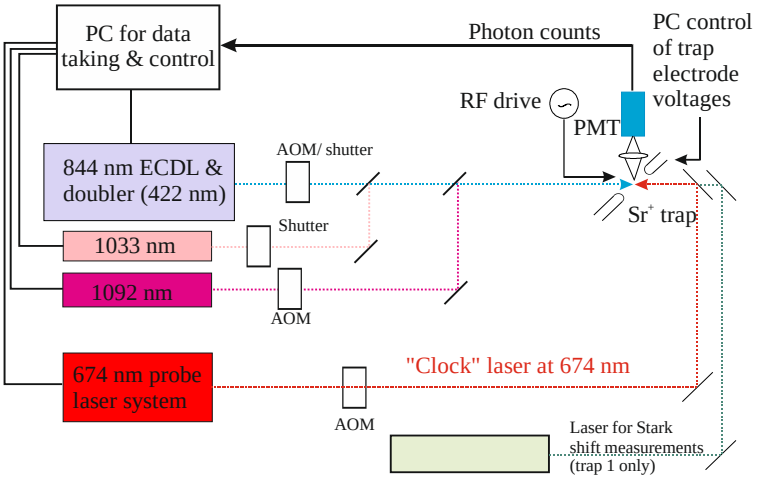

Figure 2. Overall schematic for cooling and probing $^{88}Sr^+$, with an additional laser for AC Stark shift measurements

2. Stark shift theory and measurement

The theory of Stark shifts is well-documented and tensor, vector and scalar Stark shifts can all be observed under different circumstances [8]. Both the tensor Stark shift and quadrupole shift [8, 9] vary as the square of the magnetic quantum number ($\propto m^2$) and the angle between the trap axis and the magnetic field. Interrogating and averaging over three specific pairs of Zeeman components [9, 10] eliminates both the quadrupole shift and the tensor Stark shift. A vector Stark shift [8] depends linearly on m and can be observed if some of the 674 nm light is circularly polarised. However, this is eliminated by averaging over pairs of Zeeman components symmetrically placed around line centre; this is the same routine that eliminates the first order Zeeman shift. To determine the blackbody shift, we mainly need to consider the scalar Stark shift, since blackbody radiation is normally isotropic. Where heat sources are present [12], there could be a non-isotropic electric field giving a tensor Stark shift but this is averaged out by measuring on different Zeeman components as already discussed. We therefore consider here only the scalar Stark shift.

From [6], the scalar Stark shift $\Delta\omega_{AC}$ in an electric field E for the level with total angular momentum J as a function of frequency ω is given by:

$$\Delta\omega_{AC} = \frac{E^2}{3\hbar^2(2J+1)} \sum_{J'} \frac{\omega_{JJ'} \left| < J \parallel p \parallel J' > \right|^2}{\omega_{JJ'}^2 - \omega^2} \qquad (1)$$

Here, $\left| < J \parallel p \parallel J' > \right|^2$ is a reduced dipole (p) matrix element and $\omega_{JJ'}$ is the frequency between the states J and J' listed in tables 1 and 2 of [6] with $\hbar$ the reduced Planck's constant. Equation 1 gives the shift for the $^2S_{1/2}$ ($J = \frac{1}{2}$) and $^2D_{5/2}$ ($J = \frac{5}{2}$) levels; the shift of the 674-nm clock transition is the difference between these values. For a Stark shift resulting from a laser with power P and $1/e$ amplitude radius w_0, the Stark shift can be calculated from the following relationship between the rms electric field E and the output power at the centre (i.e. point of maximum intensity) of a TEM_{00} Gaussian beam:

$$E^2 = \frac{2P}{\pi c \varepsilon_0 w_0^2} \qquad (2)$$

Substituting equation 2 into equation 1 gives values for the power shift of the $^2S_{1/2}$ and $^2D_{5/2}$ levels as a function of optical frequency ω. The difference between these values is the power shift of the 674-nm clock transition, calculated in figure 3 for w_0 = 100 μm. This figure indicates the frequencies of the 422-nm cooling transition and 1033-nm clear-out laser shown in figure 1. The wavelength at 408 nm is the 5s $^2S_{1/2}$ – 5p $^2P_{3/2}$ transition.

From measurements at different wavelengths in the region ~370 nm to ~1550 nm, we plan to experimentally verify some of the oscillator strengths of equation (1). In the initial work reported here, we observe the scalar Stark shift using a 100-mW 1064-nm fibre laser; this shift is predominantly determined by the reduced matrix element (oscillator strength) of the 4d $^2D_{5/2}$ – 5p $^2P_{3/2}$ transition at 1033 nm. Other laser wavelengths where measurements are planned are 423 nm (close to the cooling laser frequency) and 406 nm (close to the 5s $^2S_{1/2}$ – 5p $^2P_{3/2}$ transition). An additional measurement is planned in the near ultra-violet at ~370 nm. Although equation 1 contains a large number of unknowns, most of the terms from transitions in the ultra-violet can be approximated as a DC term for wavelengths longer than 400 nm. Including the transitions at 1033 nm, 422 nm and 408 nm together with one term for the closely spaced 4d $^2D_{5/2} \rightarrow$ 4f $^2F_{5/2,\ 7/2}$ uv doublet limits the number of unknowns to five. A least squares fitting routine will then be used to extract the required oscillator strengths.

Of additional interest is the determination of two "magic wavelengths", where the AC scalar Stark shift is zero; these wavelengths are calculated to be at 1545.4 nm and 417.0 nm. Both wavelengths are readily accessible; the first generated by a telecoms laser and the second either using a direct output from a blue diode or a frequency doubled 834 nm laser. The 417-nm wavelength is the equivalent to that recently measured in $^{40}Ca^{+}$ [13]. Although ion "magic wavelengths" do not have the same key significance as they do for atoms [14] they provide two additional linear relationships between the oscillator strengths independent of laser power and beam size. Uncertainty in the measurement of these two parameters is a significant contributor to the overall AC Stark shift uncertainty.

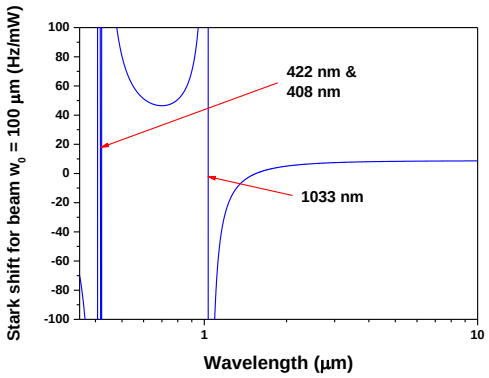

Figure 3. Calculated AC scalar Stark shifts over the wavelength region 350 nm to 10 µm for the $^{88}Sr^{+}$ 674 nm optical clock transition.

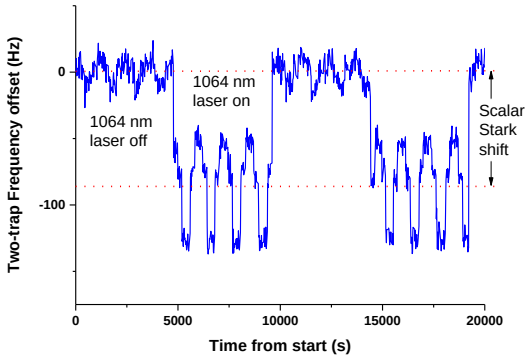

Figure 4. Stark shift observed at 1064 nm by two-trap comparison; both scalar and tensor Stark shifts are observed (see text).

Figure 4 shows our observation of the Stark shift using a 100-mW fibre laser tuned to 1064.534 nm with a 1/*e* amplitude radius (= w_0) of 600 µm. Two-trap comparison measurements are shown with the fibre laser being toggled on or off every ~80 minutes. During both the laser "on" and "off" periods, the 674-nm laser is cycled every ~3 minutes between Δm = 0, ±1 and ±2 Zeeman components. Each Zeeman component has a different quadrupole and tensor Stark shift; this accounts for the sudden frequency changes as the Zeeman component is changed. The size of these frequency steps changes when the 1064-nm laser is toggled between being on and off. This change arises from the AC tensor Stark shift at this wavelength. In order to measure the scalar Stark shift, we average the trap offset over the three Zeeman components during the periods when the 1064-nm laser is shuttered on and off (the offset with the laser shuttered off is consistent with zero).

This measurement was repeated at different 1064-nm fibre laser input beam alignments and power levels. At each power level, measurements were made at different input beam alignments, both horizontally and vertically. Since the laser output is via a single mode polarisation maintaining fibre, a spatially clean and circularly symmetric beam profile is expected; this was verified experimentally. The results for different beam alignments were fitted to a Gaussian profile to determine the frequency shift corresponding to the maximum beam intensity. For our most recent measurements, this process of beam centring has been automated by replacing the final beam-steering mirror with a type fitted with computer-controlled piezoelectric steering. The beam size was measured by placing a mirror before the trap and using a knife edge at a distance corresponding to the ion position. The accuracy of the beam-size measurement (2.5% in w_0^2; k = 1) was the largest uncertainty contribution. The frequency shift was measured at nine different powers between ~5 mW and ~18 mW and the results were fitted using linear regression. In addition to the statistical uncertainty of the regression fit, the uncertainty budget (table 1) includes contributions from uncertainties in the power including the vacuum window transmission, pointing stability and beam size determination. The result is a

measurement of the scalar Stark shift which we determine to be -5.4(2) Hz/mW for w_0 = 600 μm. Using equations 1 and 2, we calculate the expected shift as -5.51 Hz/mW, consistent with the observed result to within experimental uncertainty.

Table 1. Uncertainty budget for the Stark shift measurement at 1064 nm.

Parameter	**Relative uncertainty (k = 1)**
Beam area ($\propto w_0^2$)	2.5%
Power measurement uncertainty	1.9%
Beam pointing stability	1.6%
Regression fit	0.7%
TOTAL	3.6%

In order to use equation 1 to calculate the blackbody shift, we require the expression for the blackbody mean square electric field ξ^2 per unit bandwidth (i.e. in units of $(V/m)^2$(radian/s)$^{-1}$):

$$\xi^2 = \frac{\hbar}{\pi^2 \varepsilon_0 c^3} \frac{\omega^3}{\exp(\hbar\omega / kT) - 1} \tag{3}$$

Integrating equation 3 over all frequencies ω gives the familiar result for the total blackbody radiation field $\langle E^2 \rangle = (832\ \mathrm{V/m})^2$ at T = 300 K. To obtain the blackbody shift for the $^2S_{1/2}$ and $^2D_{5/2}$ levels, we need to substitute equation 3 into equation 1 and integrate to obtain equation 4:

$$\Delta\omega_{BB} = \frac{1}{3\hbar\pi^2\varepsilon_0 c^3 (2J+1)} \sum_{J'} \int_0^\infty \frac{\omega_{JJ'} \omega^3 |\langle J \| p \| J' \rangle|^2}{\left(\omega_{JJ'}^2 - \omega^2\right)\left(\exp\left(\frac{\hbar\omega}{kT}\right) - 1\right)} d\omega \tag{4}$$

We then sum over all the listed [6] transitions from the $^2S_{1/2}$ and $^2D_{5/2}$ levels, as indicated in equation 4. This summation also needs to include the final frequency-independent corrections listed in tables 1 and 2 of [6] to the polarisability (for example, the polarisability contribution from the electrons in the ionic core). This calculation leads to the published result for the blackbody shift, including the "dynamic correction". Once our AC Stark shift measurements at other wavelengths are complete, equation 4 could be used to update the value for the blackbody shift by replacing some of the matrix elements with their experimentally determined values.

3. Conclusion

We have presented the results of our first AC Stark shift measurements on the $^{88}Sr^+$ 674-nm optical clock transition, using a 1064-nm fibre laser. Together with future measurements planned at wavelengths close to transitions at 422 nm and 408 nm, we expect to be able to determine experimentally some of the matrix elements required to calculate the blackbody shift (equation 4). The

measurements are limited by the uncertainty of the beam size (w_0) determination; the total shift varies with the inverse square of this parameter. Of particular interest is the determination of the two accessible "magic wavelengths" for $^{88}Sr^+$ at 1545.4 nm and 417.0 nm where the AC Stark shift is calculated to be zero. These wavelengths will provide two linear relationships between the matrix elements that are independent of laser power and beam-size. The uncertainties in the measurement of these two parameters limit the accuracy of the measurement reported here. Once these measurements have been completed, a least squares fit will allow determination of the matrix elements for transitions at wavelengths longer than 400 nm; these transitions contribute most to the variation of the AC Stark shift with frequency.

Acknowledgments

This work was funded by the UK Department for Business, Innovation and Skills as part of the National Measurement System Electromagnetics and Time programme and by the European Metrology Research Programme (EMRP). The EMRP is jointly funded by the EMRP participating countries within EURAMET and the European Union.

References

[1] Barwood G P, Huang G, Klein H A, Johnson L A M, King S, Margolis H S, Szymaniec K and Gill P 2014 *Phys. Rev. A* **89**, 050501(R)
[2] Dubé P, Madej A A, Zhou Z and Bernard J E 2013 *Phys. Rev. A* **87**, 023806
[3] Barwood G P, Huang G, Klein H A and Gill P 2015 *Meas. Sci. Technol.* **26** 075203
[4] Barwood G P, Huang G, King S A, Klein H A and Gill P 2015 *J. Phys. B: At. Mol. Opt. Phys.* **48** 035401
[5] Dubé P, Madej A A, Tibbo M and Bernard J E 2014 *Phys. Rev. Lett.* **112**, 173002
[6] Jiang D, Arora1 B, Safronova M S and Clark C W 2009 *J. Phys. B: At. Mol. Opt. Phys.* **42** 154020
[7] Fordell T, Lindvall T, Dubé P, Madej A A, Wallin A E and Merimaa M 2015 *Opt. Lett.* **40** 1822
[8] Auzinsh A, Budker D and Rochester S M 2010 "*Optically Polarized Atoms: Understanding light-atom interactions*" (Oxford University Press) p 329
[9] Itano W M 2000 *J. Res. Natl. Inst. Stand. Technol.* **105**, 829
[10] Dubé P, Madej A A, Bernard J E, Marmet L, Boulanger J-S and Cundy S 2005 *Phys. Rev. Lett.* **95**, 033001
[11] Margolis H S, Barwood G P, Huang G, Klein H A, Lea S N, Szymaniec K and Gill P 2004 *Science* **306** 1355
[12] Flambaum V V, Porsev S G and Safronova M S 2016 *Phys. Rev. A* **93**, 022508
[13] Liu P-L, Huang Y, Bian W, Shao H, Guan H, Tang Y-B, Li C-B, Mitroy J and Gao K-L 2015 *Phys. Rev. Lett.* **114**, 223001
[14] Katori H and Takamoto M, Pal'chikov V G and Ovsiannikov V D 2003 *Phys. Rev. Lett.* **91**, 173005